Hindawi Publishing Corporation
Journal of Nanotechnology
Volume 2015, Article ID 848020, 8 pages
http://dx.doi.org/10.1155/2015/848020

Research Article

r_1 and r_2 Relaxivities of Dendrons Based on a OEG-DTPA Architecture: Effect of Gd^{3+} Placement and Dendron Functionalization

Peter Fransen,[1,2] Daniel Pulido,[2,3] Lorena Simón-Gracia,[1,2] Ana Paula Candiota,[2,4,5] Carles Arús,[2,4,5] Fernando Albericio,[1,2,6,7] and Miriam Royo[2,3]

[1]*Institute for Research in Biomedicine, Baldiri Reixac 10, 08028 Barcelona, Spain*
[2]*Biomedical Research Networking Center in Bioengineering, Biomaterials and Nanomedicine (CIBER-BBN), Spain*
[3]*Combinatorial Chemistry Unit, Barcelona Science Park, Baldiri Reixac 10, 08028 Barcelona, Spain*
[4]*Departament de Bioquímica i Biologia Molecular, Universitat Autònoma de Barcelona, Unitat de Biociències, Edifici C, 08193 Cerdanyola del Vallès, Spain*
[5]*Institut de Biotecnologia i de Biomedicina, Universitat Autònoma de Barcelona, 08193 Cerdanyola del Vallès, Spain*
[6]*Department of Organic Chemistry, University of Barcelona, Martí i Franquès 1-11, 08028 Barcelona, Spain*
[7]*School of Chemistry & Physics, University of KwaZulua-Natal, Durban 4001, South Africa*

Correspondence should be addressed to Fernando Albericio; albericio@irbbarcelona.org and Miriam Royo; mroyo@pcb.ub.cat

Received 23 December 2014; Revised 23 February 2015; Accepted 23 February 2015

Academic Editor: Paresh Chandra Ray

In magnetic resonance imaging, contrast agents are employed to enhance the signal intensity. However, current commercial contrast agents are hindered by a low relaxivity constant. Dendrimers can be employed to create higher molecular weight contrast agents which have an increased relaxivity due to a lower molecular rotation. In this study, dendrimers containing DTPA derivatives as cores and/or branching units were used to chelate gadolinium ions. Locating the gadolinium ions inside the dendrimers results in higher relaxivity constants, possibly because the paramagnetic center is closer to the rotational axis of the macromolecule. The highest gain in relaxivity was produced by decorating the dendron surface with peptide sequences, which could be explained by the presence of more second-sphere water molecules attracted by the peptides. These findings could contribute to the development of more effective contrast agents, either by placing the paramagnetic gadolinium ion in a strategic position or through functionalization of the dendron surface.

1. Introduction

Magnetic resonance imaging (MRI) is a widely used diagnostic tool to study the anatomy and function of the human body in both disease and health. Advantages of this imaging technique are that MRI is noninvasive, does not involve radiation, and has excellent spatial resolution [1]. However, one of the drawbacks of MRI is its relatively low sensitivity. For this reason, there is an increasing demand for more effective and specific contrast agents that help to increase the contrast between pathological and healthy tissues. This can be enhanced by using contrast agents based on Gd^{3+} that change the longitudinal relaxation rate (T_1) or by contrast agents based on superparamagnetic iron particles [2, 3] that change the transverse relaxation rate (T_2). The main mode of imaging currently employed is positive mode imaging, based on T_1 relaxivity. For bimodal imaging using both positive and negative modes (based on T_2 relaxivity), versatile contrast agents, which can enhance both relaxivity constants, are required. Such bimodal contrast agents would provide more clinical information, by combining the unique strengths of each technology and, at the same time, by reducing the adverse effects of administration of multiple agents [4]. The efficiency of both kinds of contrast agents is expressed in relaxivity constants r_1 or r_2, depending on the type of relaxivity employed. These constants describe

the relaxation rate enhancement of water protons per millimole of metal ion. The development of compounds with higher relaxivities could lead to contrast agents with higher sensitivity, which are detectable at lower doses and provide higher contrast at equivalent doses. The r_1 relaxivity can be increased by enhancing the water-exchange rate [5, 6] or by slowing down the tumbling rate of the contrast agent [7]. Dendrimers, highly branched macromolecules with a well-defined architecture, are interesting platforms for increasing the relaxivity because the increased molecular size results in a decreased molecular rotation. Furthermore, one single dendrimer molecule can be functionalized with targeting moieties or outfitted with several gadolinium ions enhancing the relaxivity even more [8, 9]. Additionally, high molecular weight macromolecules have a longer blood circulation time as compared to low molecular weight (LWH) agents with a short residence time in the vascular system [10–12].

In our research group, we have worked extensively on the synthesis and biomedical applications of dendrons which consist of a DTPA derived core unit onto which monodisperse branches of oligoethylene glycol (OEG) are conjugated. The synthesis of diverse OEG-based dendrimers has been previously described by us [13–15]. These dendrons can be grown up to generation 2 using amide bond formation or up to generation 3 by click chemistry using the copper catalyzed cycloaddition between azides and alkynes. The periphery of the dendrons consists of amine groups, which can be easily functionalized with diverse bioactive moieties such as peptides or diverse imaging agents. As was mentioned before, this type of molecules contains DTPA moieties within their structures, a widely known chelating agent [16], which can be placed in different positions of the dendron structure with diverse derivatizations. Taking into account the particular composition of these compounds, the aim of the present work was to study how the paramagnetic Gd^{3+} ion could be entrapped inside the DTPA containing architecture of the dendrons and how this would affect the relaxivity of the chelate.

2. Materials and Methods

2.1. Synthesis Dendron D1 (DTPA-1cooh-4OEG_Ac). Synthesized as previously reported in [12].

2.2. Synthesis Dendron D2 (DTPA-5OEG_Ac). DTPA bisanhydride (100 mg, 0.28 mmol) was dissolved in a mixture (7 : 3) of CH_2Cl_2/DMF (150 mL) and PyBOP (800 mg, 1.54 mmol) together with Boc-TOTA (492 mg, 1.54 mmol) was added. The basicity of the reaction mixture was adjusted to pH 8 by the addition of DIEA. The reaction was allowed to stir for 1 hour at room temperature, after which the solvent was concentrated under reduced pressure. The crude product was dissolved in 50 mL of CH_2Cl_2 and washed three times with 5% $NaHCO_3$ (50 mL). The crude product was dissolved in 10 mL of CH_2Cl_2 and transferred to a 50 mL falcon tube. Hexane (40 mL) was added and the falcon was vigorously shaken and centrifuged. The supernatant was discarded and the precipitated pellet corresponded to the crude product. The crude was purified by flash chromatography over basic aluminum oxide eluting with 1% MeOH in DCM to yield the pure Boc-protected dendron (450 mg, 85%). ^{1}H NMR (400 Mhz, $CDCl_3$): δ = 1.36 (s, 45 H), 1.70 (m, 20 H), 2.57 (m, 8 H), 3.03 (s, 2 H), 3.06–3.17 (m, 18 H), 3.26 (m, 10 H), 3.46 (m, 20 H), 3.50–3.60 (m, 50 H), and 7.76 (bs, NH). ^{13}C NMR (100 MHz, $CDCl_3$): δ = 28.40, 29.32, 29.64, 36.87, 38.26, 46.20, 53.06, 58.39, 59.11, 69.13, 69.29, 70.05, 70.07, 70.36, 70.39, 78.82, 156.07, and 170.82. MS: Theoretical mass for $[C_{89}H_{173}N_{13}O_{30}]^+$: 1905.2489. Experimental mass detected by LC-MS: 954.46 (M+2)/2. Experimental mass detected by HRMS (ES^+): 1905.2437.

The Boc-terminated dendron (180 mg, 0.095 mmol) was dissolved in 5 mL of TFA/H_2O (95 : 5) and stirred for 1 hour at room temperature. Subsequently, the TFA was evaporated using a flow of N_2 and the product was precipitated in methyl *tert*-butyl ether in order to remove the carbocations generated during the deprotection. After decanting the methyl *tert*-butyl ether, the pellet containing the deprotected dendrimer was dissolved in 5 mL CH_2Cl_2 and DIEA (0.63 mmol, 111 μL) and Ac_2O (0.52 mmol, 49 μL) were added. The reaction was allowed to stir for 2 hours at room temperature, and then hexane (40 mL) was added. The mixture was stirred vigorously and centrifuged. The supernatant was discarded and the remaining oily precipitate corresponded to pure compound **D2** (167 mg, 89%). ^{1}H NMR (400 Mhz, $CDCl_3$): δ = 1.70 (m, 20 H), 1.89 (s, 15 H), 2.69 (m, 4 H), 2.79 (m, 4 H), 3.17 (s, 8 H), 3.23 (m, 20 H), 3.34 (s, 2 H), 3.45–3.49 (m, 20 H), 3.50–3.58 (m, 50 H), and 8.03 (bs, NH). ^{13}C NMR (100 MHz, $CDCl_3$): δ = 28.83, 29.25, 36.77, 37.52, 52.37, 53.05, 58.76, 68.94, 69.50, 69.90, 69.96, 70.28, 170.94, and 171.15. MS: Theoretical mass for $[C_{74}H_{143}N_{13}O_{25}]^+$: 1615.0397. Experimental mass detected by LC-MS: 809.15 (M+2)/2. Experimental mass detected by HRMS (ES^+): 1615.0354.

2.3. Synthesis Dendron D3 (DTPA-1OEG_NH2-4OEG_peptide). The dendron DTPA-1coobn-4OEG_Boc (synthesis reported in [12]) (600 mg, 0.24 mmol) was dissolved in 50 mL MeOH. The heterogenous catalyst 10% wt Pd/C was added (40 mg) and the flask was purged with N_2 and then with H_2. The reaction was stirred for 2 hours at room temperature under H_2 atmosphere, and then the flask was purged again with N_2. The catalyst was removed by filtration over Celite and washed with ethyl acetate (3 × 15 mL). The organic phase, consisting of MeOH and ethyl acetate, was evaporated to yield yellowish oil. This oil was dissolved with CH_2Cl_2/DMF (7 : 3, v/v; 100 mL) and PyBOP (135 mg, 0.26 mmol) together with 13-azido-4,7,10-trioxatridecaneamine (NH_2-OEG-N_3; 65 mg, 0.26 mmol) was added. The basicity of the reaction mixture was adjusted to pH 8 by the addition of DIEA. The reaction was allowed to stir for 1 hour at room temperature, and then the solvent was concentrated under reduced pressure. The crude product was dissolved in 50 mL of CH_2Cl_2 and washed three times with 5% $NaHCO_3$ (50 mL). The organic phase was dried with $MgSO_4$, and the volume was reduced to 10 mL and transferred to a 50 mL falcon tube. Hexane (40 mL) was added and the falcon was vigorously shaken and centrifuged. The supernatant was discarded and the precipitated pellet

corresponded to the crude product. The crude was purified by flash chromatography over basic aluminium oxide eluting with 1% MeOH in DCM to yield the pure dendron (389 mg, 91%). ^{1}H NMR (400 MHz, $CDCl_3$): δ = 1.39 (s, 36 H), 1.67–1.83 (m, 20 H), 2.52–2.86 (m, 8 H), 3.05 (bs, 2 H), 3.08–3.21 (m, 16 H), 3.25–3.33 (m, 10 H), 3.55 (*t*, J = 6.70 Hz, 2 H), 3.48 (*t*, J = 6.30, 20 H), 3.52-3.62 (m, 40 H), and 7.65 (bs, NH). ^{13}C NMR (100 MHz, $CDCl_3$): δ = 28.41, 29.05, 29.37, 29.67, 37.05, 38.37, 48.37, 53.13, 53.41, 59.12, 69.30, 70.10, 70.12, 70.42, 70.44, 78.84, 156.04, and 170.67. HPLC: 5 → 100% acetonitrile (0.036% TFA) in water (0.045% TFA) over 8 min (SunFire C_{18}), t_R = 6.55 min. MS: Theoretical mass for $[C_{84}H_{163}N_{15}O_{28}+H]^+$: 1831.1865. Experimental mass detected by HPLC-MS: 916.55 (M+2)/2. Experimental mass detected by HRMS (ES^+): 1831.1906.

The dendron platform DTPA-1OEG_N_3-4OEG_Boc (100 mg, 0.055 mmol) was dissolved in 5 mL 4 M HCl in dioxane and stirred at room temperature overnight. Then, dioxane was evaporated to dryness. The crude was dissolved in 100 mL of CH_2Cl_2/DMF (7 : 3, v/v) and PyBOP (124 mg, 0.24 mmol) together with Ac-NH-Asp(tBu)-Gly-Ser (tBu)-Arg(Pbf)-OH (201 mg, 0.24 mmol) was added. The basicity of the reaction mixture was adjusted to pH 8 by the addition of DIEA. The reaction was allowed to stir for 1 hour at room temperature, and then the solvent was concentrated under reduced pressure. The crude product was dissolved in 20 mL of CH_2Cl_2 and washed three times with 5% $NaHCO_3$ (20 mL). The organic phase was dried with $MgSO_4$ and evaporated to yield the peptide functionalized dendron. This compound was dissolved in 5 mL of a mixture of EtOH/H_2O (7 : 3, v/v) and NH_4Cl (6 mg, 0.13 mmol) and fine zinc powder (5 mg, 0.072 mmol) were added. The suspension was magnetically stirred for several hours until the colour of the suspension turned to a lighter grey, indicating the oxidation of the zinc particles. Completion of the reaction was confirmed by HPLC-PDA and HPLC-MS. After completion, the EtOH was removed *in vacuo*. The crude was transferred to a 50 mL falcon tube using CH_2Cl_2 (40 mL). The falcon was vigorously shaken and centrifuged, thereby precipitating the salts. The supernatant was collected and evaporated to yield the crude peptide functionalized dendron. The side-chain protecting groups were removed by dissolving the pellet in 4 mL of TFA/H_2O/TIS (95 : 2.5 : 2.5). After 1 hour of reaction at room temperature, the TFA was removed using a flow of N_2 and the compound was precipitated in cold *tert*-butyl methyl ether. The precipitate was dissolved in 4 mL of H_2O and dialyzed for several hours using a dialysis membrane with MWCO 1 kDa to yield the final product **D3** (55 mg, 30%). ^{1}H NMR (400 Mhz, $CDCl_3$): δ = 1.40–1.59 (m, 8 H), 1.65 (m, 20 H), 1.72–1.88 (m, 8 H), 1.93 (s, 12 H), 2.72 (m, 8 H), 2.97 (m, 4 H), 3.09 (m, 12 H), 3.16 (m, 10 H), 3.27 (m, 8 H), 3.43 (m, 20 H), 3.54 (m, 40 H), 3.78 (m, 8 H), 3.80–4.00 (m, 16 H), 4.17 (m, 4 H), 4.30 (*t*, J = 4.53 Hz, 4 H), and 6.55 (*t*, J = 6.24 Hz, 4 H). ^{13}C NMR (100 MHz, $CDCl_3$): δ = 21.62, 24.25, 27.87, 28.04, 28.13, 30.16, 35.17, 36.30, 40.42, 42.52, 49.99, 53.64, 56.03, 60.90, 68.06, 69.24, 69.31, 69.47, 156.63, 171.12, 171.38, 172.27, 173.85, 174.43, and 174.63. HPLC: 0 → 60% acetonitrile (0.036% TFA) in water (0.045% TFA) over 8 min (SunFire C_{18}), t_R = 4.61 min. MS: Theoretical mass for $[C_{132}H_{241}N_{41}O_{52}]^+$: 3232.7469. Experimental mass detected by HPLC-MS: 809.67 (M+4)/4, 647.95 (M+5)/5, 540.03 (M+6)/6. Experimental mass detected by HRMS (ES^+): 3232.7513.

2.4. Synthesis of the Peptide Ac-NH-Asp(tBu)-Gly-Ser(tBu)-Arg(Pbf)-OH. The solid-phase synthesis was carried out manually on 50 mL polypropylene syringes, using standard protocols described for solid-phase peptide synthesis. Standard amino acid couplings were performed with OxymaPure/DIPCDI. After incorporation of the fourth and final amino acid, the Fmoc-group was removed and the amino group was acetylated using acetic anhydride (944 μL, 10 mmol) and DIEA (3860 μL, 20 mmol). The peptide was cleaved from the resin with 1% TFA in DCM (20 × 2 min) and the resin was ultimately washed with DCM (5 × 2 min). The washings were collected in 200 mL of DCM. The organic phase was evaporated and the protected peptide was dissolved in 50 mL of ACN/H_2O (1 : 1) and lyophilized. HPLC: 5 → 100% acetonitrile (0.036% TFA) in water (0.045% TFA) over 8 min (SunFire C_{18}), t_R = 6.68 min. MS: Theoretical mass for $[C_{38}H_{61}N_7O_{12}S]^+$: 839.4099. Experimental mass detected by HPLC-MS: 840.78 (M+H).

2.5. Synthesis Dendron D4. Synthesized as previously reported in [15].

2.6. Synthesis Dendrons D5 and D6. Synthesized as previously reported in [13].

2.7. Formation of Gadolinium-Dendron Complexes. The dendrons were dissolved in water and $GdCl_3$ was added (1.2 eq per chelating moiety). The pH of the solution was adjusted to 7 and the mixture was incubated overnight at room temperature. Then, the excess of Gd^{3+} (nonchelated) was removed from the final samples by dialysis. The samples were dialyzed several times until Gd^{3+} was not detected in the external dialysis media and dialyzed again one more time. The presence of Gd^{3+} in the external dialysis media was checked by the use of xylenol orange, a widely sensitive indicator for heavy metals. The final complexes were lyophilized and analyzed HPLC-MS to verify full complex formation.

2.8. Phantom MRI Studies

2.8.1. MRI Acquisition. The gadolinium-dendron complexes were dissolved in distilled water, in concentrations ranging from 0.125 to 2 mM in gadolinium (Gd^{3+}). Solutions were placed in round bottom vials, which were immobilized in a polystyrene foam support used for the MRI measurements. MRI images of the phantoms were acquired in sagittal, coronal, and transversal planes at 22.4 ± 0.4°C. These studies were carried out on a 7*T* horizontal magnet (BioSpec 70/30 USR; Bruker BioSpin, Ettlingen, Germany) at the Joint NMR Facility of the Universitat Autònoma de Barcelona and CIBER-BBN (Cerdanyola del Vallès, Spain). This magnet

was equipped with actively shielded gradients (B-GA12 gradient coil inserted into a BGA20S gradient system) and a quadrature probe of 7.2 cm diameter was used for these acquisitions. The experimental parameters for the T_2-weighted (T_2w) spin-echo images were rapid acquisition with relaxation enhancement and variable repetition time (RAREVTR), sequence with repetition time (TR) of 4,000 ms, effective echo time (TEeff) of 20 ms, rare factor of 1, number of averages (NA) = 1, matrix (MTX): 256 × 128, field of view (FOV): 110 × 55 mm (0.43 mm/pixel), slice thickness of 2 mm, and total acquisition time of 8 min 32 sec. The parameters for the T_1-weighted image (T_1w) were rapid acquisition with relaxation enhancement and variable repetition time (RAREVTR), TR: 100 ms, T_{eff}: 6 ms, NA= 16, MTX: 256 × 128, FOV: 110 × 55 mm (0.43 mm/pixel), slice thickness of 2 mm, and total acquisition time of 3 min 24 sec. For T_2 measurements, a multislice multiecho (MSME) sequence was used, with TR of 5,000 ms, echo times between 10 and 640 ms in steps of 10 ms (total = 64 echoes), MTX: 128 × 128, FOV of 110 × 55 mm (0.859 and 0.430 mm/pixel), slice thickness of 2 mm, and total acquisition time of 10 min 40 sec. For T_1 measurements, a RAREVTR sequence was used, with T_{eff}: 6 ms, variable TR (50/80/120/160/200/250/300/360/420/500/650/850/1,100/1,600/2,200/3,000/5,000/10,000 ms), MTX: 128 × 64, FOV: 110 × 55 mm (0.859 mm/pixel), slice thickness of 2 mm, and total acquisition time of 28 min 37 sec.

2.8.2. Data Processing. For T_1 and T_2 calculations for each compound, three different regions of interest (ROIs) were manually defined inside each phantom vial, for each concentration point, after visual inspection of the images acquired for T_1 and T_2 measurements, in the coronal plane. Image analysis was carried out with Bruker software Paravision (version 4.0). The inverse of the calculated T_1 and T_2 values ($1/T_1$ and $1/T_2$) was plotted against Gd concentration for each experimental point, and the slope of the line corresponded to the compound relaxivity (s^{-1} mM^{-1}).

2.9. Statistical Analysis. Normality of the data was first inspected in each group by the Kolmogorov-Smirnov test and variance homogeneity with the Levene test. Two-tailed student's t-test for independent measurements was used for statistical analysis and the significance level for all tests was set to $P < 0.05$.

3. Results and Discussion

In light of the aforementioned objective, six different dendrons were synthesized (see Figure 1). Compound **D1** is a first generation dendron, prepared from a bifunctional orthogonally protected DTPA core, which contains acetylated amines on its surface. Compound **D2** is a first generation dendron with 5 OEG-Ac branches and it was synthesized using the commercially available DTPA bisanhydride. Compound **D3** was prepared by conjugating a short DGSR peptide onto an orthogonally protected derivative of **D2**. Compound **D3** was included in the study to see whether the functionalization of the periphery would influence the relaxivity. Compound **D4** is a second generation dendron constructed by means of amide bonds [15]. And finally compounds **D5** and **D6** are the second and third generation dendrons, respectively, constructed from the corresponding first generation dendron through a two-step process of diazo transfer and click chemistry reactions; thus, the dendrimer growth is achieved through triazole bonds [13].

The first step was to explore how the different DTPA containing dendritic structures were able to chelate gadolinium. The chelating capacity of the different dendritic structures was studied using HPLC-PDA and HPLC-MS after incubation of the dendrons in an aqueous solution of $GdCl_3$ at pH 7. Analysis by mass spectrometry clearly showed the mass of the dendron-metal complex and allowed us to distinguish between Gd^{3+}-dendron complex and free dendron. After complete complex formation was observed, the excess of Gd^{3+} was removed by several dialysis processes and final complex confirmed by HPLC-MS and HPLC-PDA. Using mass spectrometry technique, it was found that the chelation was influenced heavily by the derivation of the DTPA moiety (see Figure 2). For instance, the first generation dendron with a benzyl ester in the focal point (**D1** derivative) was not able to chelate gadolinium. The term focal point refers to the functional group in the center of the DTPA moiety. However, when the benzyl group was replaced by an amide moiety (**D2** and **D3**) or a free carboxylic acid (**D1**), the dendron was able to chelate gadolinium.

For the higher generation dendrons, their chelating capacity depends on the framework of the dendron, that is, triazole moiety (**D5** and **D6**) or amide bond (**D4**). For example, in second generation dendrons, the four DTPA moieties in the apical positions (DTPA moieties of the branching units) did not chelate gadolinium when containing triazole rings (**D5** and **D6**). Gadolinium chelation did occur when the second generation dendron framework was composed of amide bonds (**D4**) instead of the triazole rings. This means that this amide-type architecture has a higher gadolinium payload.

In order to see how the dendritic architecture of the dendron-gadolinium would influence the distribution of the paramagnetic effect of the gadolinium ion, we measured the water proton relaxation rates T_1 and T_2 at a concentration range of 0.125–2 mM of chelated Gd^{3+} in water. The relaxivities r_1 and r_2 were calculated by determining the slope of the regression line of $1/T_1$ and $1/T_2$ versus the concentration with a least-squares method. The relaxivities r_1 and r_2 for the different types of dendron-metal complex are given in Table 1. The commercially available contrast agent DOTAREM was used as a reference.

3.1. r_1 Relaxivity. As can be seen in the measured relaxivities for **D1**, **D5,** and **D6**, containing the gadolinium ion in the barycenter of the OEG-based dendron indeed had a positive effect on the relaxation rate. As expected, this effect is a result of the increased size of the dendrons, which together with the placement of the metal in the barycenter decreased the overall tumbling rate of the dendron-metal complex.

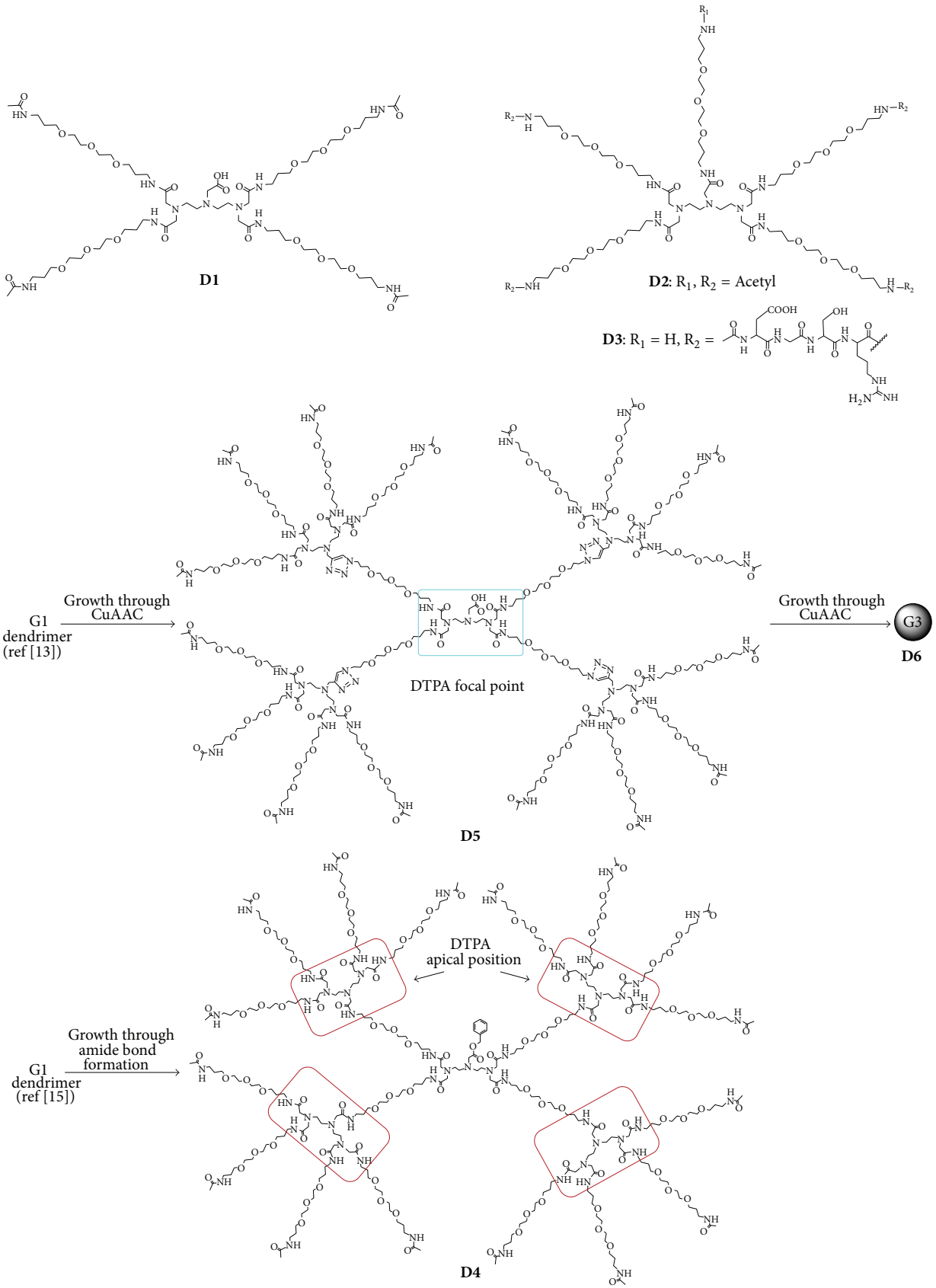

Figure 1: Molecular structures of the different OEG-DTPA dendrons used in this study. The central DTPA moiety is indicated in blue whereas the apical DTPA moieties are indicated in red.

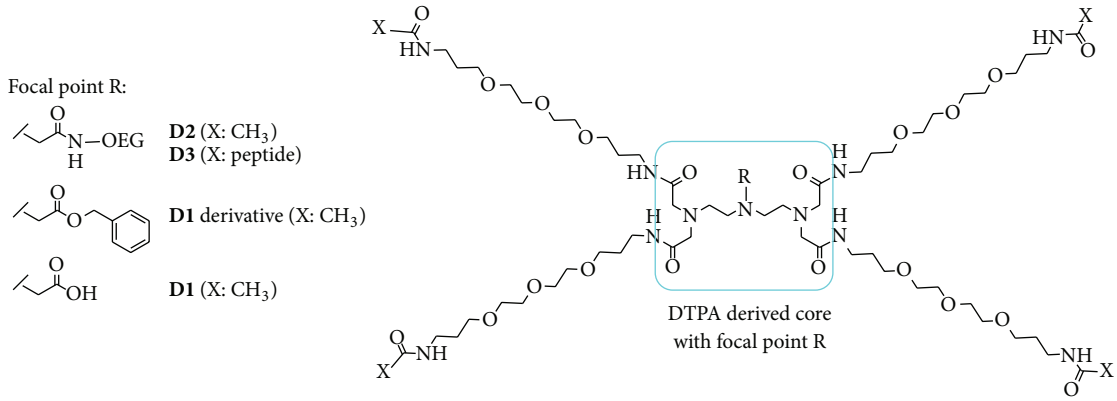

Figure 2: Molecular structure of first generation OEG-DTPA dendron. The focal point of the DTPA moiety is indicated with R and can consist of several functional groups.

Table 1: Relaxivities r_1 and r_2 per Gd^{3+} of different dendrons.

Compound	r_1 (mM^{-1} s^{-1})	r_2 (mM^{-1} s^{-1})	r_2/r_1
DOTAREM	4.00 ± 0.59	4.69 ± 0.33	1.17
D1	4.24 ± 0.07	5.14 ± 0.08$^{\$}$	1.21
D2	3.98 ± 0.07	5.55 ± 0.54$^{\$}$	1.39
D3	35.15 ± 1.40*	40.48 ± 0.84*	1.15
D4	16.08 ± 0.18*	22.43 ± 0.42*	1.39
D5	8.45 ± 0.31*	11.44 ± 0.45*	1.35
D6	12.28 ± 0.05*	24.56 ± 0.62*	2.00

$^{*}P < 0.05$ for comparisons with DOTAREM; $^{\$}P < 0.1$ for comparisons with DOTAREM.

The first generation dendron (**D1**) produced a nonsignificant increase ($P > 0.05$) as compared to DOTAREM, but the larger second (**D5**) and third generation (**D6**) dendrons gave a significant twofold and threefold increase, respectively, in the longitudinal relaxation rate (r_1). The increase in relaxivity (4.2–12.3 mM^{-1} s^{-1} at 7*T*) was not as high as compared to the values reported by Fulton and coworkers for their polysaccharide or oligoethylene glycol based dendritic structures in which the gadolinium ion was placed in the barycenter as well (ca. 27 mM^{-1} s^{-1} at about 3*T*) [17, 18]. Since the size of our higher generation dendrons is similar or even higher than that of the molecules described by Fulton and colleagues, other explanations should be considered to account for those differences. Then, the well-known decrease of r_1 with field strength [19] could possibly explain most of the recorded differences. Indeed, a factor of ca. 3-fold decrease in r_1 has been described for nanoparticulated Gd quelates between 1.4 and 7*T* [20]. Still, additional contributions could come from the fact that compounds described in [18] were glyconjugates, providing second-sphere water molecules close to the chelated Gd, with increased bulk relaxivity. This feature was absent in the dendron structures described in this work.

The second generation dendron based on an amide framework (**D4**) also exhibited a higher relaxation rate of 16.08 $mmol^{-1}$ s^{-1} per gadolinium ion, four times greater than DOTAREM. This means that trapping the gadolinium ion in the amide apical centers, which are the branching units between the central core and the periphery of the dendron, also has a positive effect on the relaxivity. This effect seems to be even greater than when Gd^{3+} is situated in the barycenter. Placement of a gadolinium ion in the apical centers has the advantage of an increased cargo load (4 Gd^{3+} ions) compared to placement in the barycenter (1 Gd^{3+}) and a total relaxivity (r_1) of 64.40 mM^{-1} s^{-1} per dendron molecule. Compared to other dendrimer structures (i.e., PAMAM; r_1 = 30 mM^{-1} s^{-1} per dendron molecule) which carry the gadolinium-ligand complex at the periphery [12], the gadolinium placed in the amide apical center is closer to the core of the dendrimer and its axis of motion. This helps to decrease the overall rotation of the gadolinium ion and then promote higher relaxivity, similarly as with placement in the barycenter. Therefore, placement in the amide apical center offers an elegant option to load a dendron with multiple gadolinium ions. At the same time, the periphery of the dendron is available for decoration with any desired functional moiety.

The most dramatic increase in the relaxivity constant r_1 was caused by the dendron **D3**, the first generation dendron outfitted with four peptide DGSR sequences. The relaxivity was increased by a factor of 8-9 as compared to the other first generation dendrons, even though the molecular weight of the peptide-dendron conjugate was only 1.5 times higher. Therefore, the small increase in molecular weight could not be used to explain the large increase in relaxivity. A possible contribution to the relaxivity gain could arise from the formation of a hydrogen-bonded network of second-sphere water molecules attracted by the polar residues of the peptide sequences [18, 21, 22]. An additional favorable aspect may be an r_2/r_1 ratio within the expected for classical T_1 agents (1.15), very similar to the one of DOTAREM (1.17).

3.2. r_2 Relaxivity. Due to the decreased rotation of the gadolinium ion imposed by the dendrimer structure, the relaxivity constant r_1 increased. But as can be seen in Table 1, there is the added feature of an increase in the r_2 constant as well. The increase in the r_2 constant follows a similar pattern as the increase of the r_1 constant, with again compound

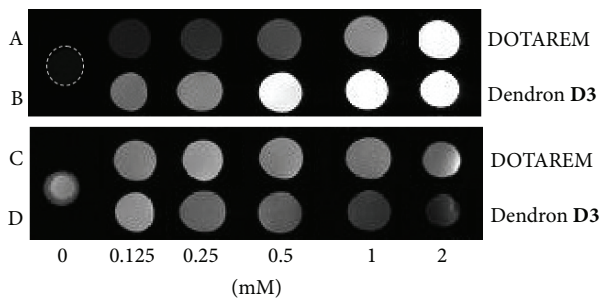

Figure 3: MRI acquisitions at 7.0T of the phantom samples used for relaxivity calculation. Rows A and C show DOTAREM solutions (T_1 and T_2 weighted MRI acquisitions, resp.) at increasing Gd^{3+} concentration listed below the figure, while rows B and D show **D3** solutions at the same concentrations/conditions as for DOTAREM, except by 0 mM (pure water). There was only one 0 mM (no CA) phantom tube. The faint image corresponding to 0 mM is outlined with a dotted white line in the T_1 weighted acquisitions for better visualization.

D3 showing the most dramatic and statistically significant increase in comparison with DOTAREM relaxivity values. In the literature, some research has been reported about simultaneous increases in both relaxivity constants r_1 and r_2 This was accomplished either by entrapping DOTAREM in hydrogel nanoparticles [23] or by outfitting polyamide dendrimers with hydroxypyridinone (HOPO) complexes [24, 25]. In the first report [23] related to hydrogel nanoparticles, the improvement in the relaxivity was attributed by the authors to both the restriction of the rotational motion of the gadolinium complex and the highly hydrated nature of the hydrogel network, which enhances the outer-sphere water molecule interactions and effectively transfers magnetic effect to the bulk water. This previous principle was also used to explain the higher r_2 relaxivity of polyamide dendrimers with HOPO [24, 25], where the outer-sphere water exchange plays a large role in T_2 relaxation. Therefore, the increased r_2 relaxivity induced by the OEG-based dendrons shown in this work might also be explained by the hydrophilic character of the molecules, which gives rise to a higher number of hydrogen bonded second and outer-sphere water molecules.

3.3. Phantom Studies at 7.0T. In order to better visualize how the changes in relaxivity values were translated into contrast, both T_1 and T_2 weighted images of the phantom containing solutions of dendrons and DOTAREM acquired at 7T for relaxivity calculation are shown (Figure 3, A–D, DOTAREM versus dendron **D3**). In the T_1 weighted images, signal enhancement clearly increased with the Gd^{3+} concentration, whereas, in the T_2 weighted images, a signal decrease (darkening) was observed with the increase of gadolinium concentration. The comparison with controls (no contrast agent added) confirmed that the enhancement of the signal, both positive and negative, was only observed in dendrons or DOTAREM solutions. Figure 3 (dendron **D3**) also shows clearly that the contrast enhancement obtained is better than the one obtained with DOTAREM, both for T_1 and T_2 weighted images. Overall, these studies corroborated the changes observed in relaxometric values and also pointed to the dual properties of the studied dendrons.

4. Conclusion

In this study, we examined how the architecture and functionalization of dendrons based on DTPA branching units influenced the relaxivity properties of the dendron-gadolinium complexes. It was found that, as expected, the increased size of the second and third generation dendrons significantly enhanced the relaxivity due to the decreased tumbling rate of the contrast agent complex when placing the paramagnetic gadolinium ion in the barycenter. An added effect of the OEG-based dendrons is their hydrophilic nature, which causes the relaxivity r_2 to be increased as well. Furthermore, the periphery of the dendrons can be decorated with functional moieties of distinct natures, for instance peptides, which can be used for active targeting or even to enhance the relaxivity constants r_1 and r_2 even more. The simultaneous increase in the relaxivity constants r_1 and r_2 could be used to develop contrast agents for dual mode imaging, which can give complementary information to single contrast type agents.

Conflict of Interests

The authors declare that there is no conflict of interests regarding the publication of this paper.

Acknowledgments

The authors thank the Peptide Synthesis Unit of the Bioengineering Biomaterial and Nanomedicine Networking Center at Barcelona Science Park for supplying peptide material used in this work. This work was partially supported by the Spanish Government MINECO (SAF2011-30508-C02-01 (MR), CTQ2012-30930 (FA), and SAF 2011–23870 (APC and CA)) and *Centro de Investigación Biomédica en Red–Bioingeniería, Biomateriales y Nanomedicina* (CIBER-BBN, [http://www.ciber-bbn.es/en]), an initiative of the Instituto de Salud Carlos III (Spain) cofunded by EU FEDER funds. The Generalitat de Catalunya (2014SGR137 and 2014SGR191) and *La Caixa* Social Program (PF) are also acknowledged for their financial support.

References

[1] P. Caravan, "Strategies for increasing the sensitivity of gadolinium based MRI contrast agents," *Chemical Society Reviews*, vol. 35, no. 6, pp. 512–523, 2006.

[2] S. Cavalli, D. Carbajo, M. Acosta et al., "Efficient γ-aminoproline-derived cell penetrating peptide-superparamagnetic iron oxide nanoparticle conjugates via aniline-catalyzed oxime chemistry as bimodal imaging nanoagents," *Chemical Communications*, vol. 48, no. 43, pp. 5322–5324, 2012.

[3] S. Laurent, D. Forge, M. Port et al., "Magnetic iron oxide nanoparticles: synthesis, stabilization, vectorization, physicochemical characterizations and biological applications," *Chemical Reviews*, vol. 108, no. 6, pp. 2064–2110, 2008.

[4] H. Yang, Y. Zhuang, Y. Sun et al., "Targeted dual-contrast T1- and T2-weighted magnetic resonance imaging of tumors using multifunctional gadolinium-labeled superparamagnetic iron oxide nanoparticles," *Biomaterials*, vol. 32, no. 20, pp. 4584–4593, 2011.

[5] S. Laurent, L. Vander Elst, F. Botteman, and R. N. Muller, "An assessment of the potential relationship between the charge of Gd-DTPA complexes and the exchange rate of the water coordinated to the metal," *European Journal of Inorganic Chemistry*, vol. 2008, pp. 4369–4379, 2008.

[6] S. Laus, R. Ruloff, É. Tóth, and A. E. Merbach, "GdIII complexes with fast water exchange and high thermodynamic stability: potential building blocks for high-relaxivity MRI contrast agents," *Chemistry*, vol. 9, no. 15, pp. 3555–3566, 2003.

[7] C.-T. Yang and K.-H. Chuang, "Gd(iii) chelates for MRI contrast agents: from high relaxivity to 'smart', from blood pool to blood-brain barrier permeable," *MedChemComm*, vol. 3, no. 5, pp. 552–565, 2012.

[8] K. Luo, G. Liu, B. He et al., "Multifunctional gadolinium-based dendritic macromolecules as liver targeting imaging probes," *Biomaterials*, vol. 32, no. 10, pp. 2575–2585, 2011.

[9] L. Han, J. Li, S. Huang et al., "Peptide-conjugated polyamidoamine dendrimer as a nanoscale tumor-targeted T1 magnetic resonance imaging contrast agent," *Biomaterials*, vol. 32, no. 11, pp. 2989–2998, 2011.

[10] H. Kobayashi and M. W. Brechbiel, "Dendrimer-based nanosized MRI contrast agents," *Current Pharmaceutical Biotechnology*, vol. 5, no. 6, pp. 539–549, 2004.

[11] M. Longmire, P. L. Choyke, and H. Kobayashi, "Dendrimer-based contrast agents for molecular imaging," *Current Topics in Medicinal Chemistry*, vol. 8, no. 14, pp. 1180–1186, 2008.

[12] A. R. Menjoge, R. M. Kannan, and D. A. Tomalia, "Dendrimer-based drug and imaging conjugates: design considerations for nanomedical applications," *Drug Discovery Today*, vol. 15, no. 5-6, pp. 171–185, 2010.

[13] P. Fransen, D. Pulido, C. Sevrin, C. Grandfils, F. Albericio, and M. Royo, "High control, fast growth OEG-based dendron synthesis via a sequential two-step process of copper-free diazo transfer and click chemistry," *Macromolecules*, vol. 47, no. 8, pp. 2585–2591, 2014.

[14] D. Pulido, F. Albericio, and M. Royo, "Controlling multivalency and multimodality: up to pentamodal dendritic platforms based on diethylenetriaminepentaacetic acid cores," *Organic Letters*, vol. 16, no. 5, pp. 1318–1321, 2014.

[15] L. Simón-Gracia, D. Pulido, C. Sevrin, C. Grandfils, F. Albericio, and M. Royo, "Biocompatible, multifunctional, and well-defined OEG-based dendritic platforms for biomedical applications," *Organic & Biomolecular Chemistry*, vol. 11, no. 24, pp. 4109–4121, 2013.

[16] S. Laurent, C. Henoumont, L. Vander Elst, and R. N. Muller, "Synthesis and physicochemical characterisation of Gd-DTPA derivatives as contrast agents for MRI," *European Journal of Inorganic Chemistry*, no. 12, pp. 1889–1915, 2012.

[17] D. A. Fulton, M. O'Halloran, D. Parker, K. Senanayake, M. Botta, and S. Aime, "Efficient relaxivity enhancement in dendritic gadolinium complexes: effective motional coupling in medium molecular weight conjugates," *Chemical Communications*, no. 4, pp. 474–476, 2005.

[18] D. A. Fulton, E. M. Elemento, S. Aime, L. Chaabane, M. Botta, and D. Parker, "Glycoconjugates of gadolinium complexes for MRI applications," *Chemical Communications*, no. 10, pp. 1064–1066, 2006.

[19] P. Caravan, C. T. Farrar, L. Frullano, and R. Uppal, "Influence of molecular parameters and increasing magnetic field strength on relaxivity of gadolinium- and manganese-based T1 contrast agents," *Contrast Media and Molecular Imaging*, vol. 4, no. 2, pp. 89–100, 2009.

[20] A. P. Candiota, M. Acosta, R. V. Simões et al., "A new ex vivo method to evaluate the performance of candidate MRI contrast agents: a proof-of-concept study," *Journal of Nanobiotechnology*, vol. 12, no. 1, article 12, 2014.

[21] J. Rudovský, P. Hermann, M. Botta, S. Aime, and I. Lukes, "Dendrimeric Gd(III) complex of a monophosphinated DOTA analogue: optimizing relaxivity by reducing internal motion," *Chemical Communications*, no. 18, pp. 2390–2392, 2005.

[22] M. Botta, "Second coordination sphere water molecules and relaxivity of gadolinium(III) complexes: implications for MRI contrast agents," *European Journal of Inorganic Chemistry*, no. 3, pp. 399–407, 2000.

[23] T. Courant, V. G. Roullin, C. Cadiou et al., "Hydrogels incorporating GdDOTA: towards highly efficient dual T 1/T2 MRI contrast agents," *Angewandte Chemie—International Edition*, vol. 51, no. 36, pp. 9119–9122, 2012.

[24] P. J. Klemm, W. C. Floyd III, C. M. Andolina, J. M. J. Frechet, and K. N. Raymond, "Conjugation to biocompatible dendrimers increases lanthanide relaxivity of hydroxypyridinone (HOPO) complexes for magnetic resonance imaging (MRI)," *European Journal of Inorganic Chemistry*, vol. 2012, no. 112, pp. 2108–2114, 2012.

[25] P. J. Klemm, W. C. Floyd, D. E. Smiles, J. M. J. Fréchet, and K. N. Raymond, "Improving T1 and T2 magnetic resonance imaging contrast agents through the conjugation of an esteramide dendrimer to high-water-coordination Gd(III) hydroxypyridinone complexes," *Contrast Media and Molecular Imaging*, vol. 7, no. 1, pp. 95–99, 2012.